Development/Plasticity/Repair

Postnatal Neurogenesis and Gliogenesis in the Olfactory Bulb from NG2-Expressing Progenitors of the Subventricular Zone

Adan Aguirre and Vittorio Gallo
Center for Neuroscience Research, Children's Research Institute, Children's National Medical Center, Washington, DC 20010

We used a 2′,3′-cyclic nucleotide 3′-phosphodiesterase (CNP)–enhanced green fluorescent protein (EGFP) transgenic mouse to study postnatal subventricular zone (SVZ) progenitor fate, with a focus on the olfactory bulb (OB). The postnatal OB of the CNP–EGFP mouse contained EGFP$^+$ interneurons and oligodendrocytes. In the anterior SVZ, the majority of EGFP$^+$ progenitors were NG2$^+$. These NG2$^+$/EGFP$^+$ progenitors expressed the OB interneuron marker Er81, the neuroblast markers doublecortin (DC) and Distalless-related homeobox (DLX), or the oligodendrocyte progenitor marker Nkx2.2. In the rostral migratory stream (RMS), EGFP$^+$ cells displayed a migrating phenotype. A fraction of these cells were either NG2$^-$/Er81$^+$/DC$^+$/DLX$^+$ or NG2$^+$/Nkx2.2$^+$. DiI (1,1′-dioctadecyl-3,3,3′,3′-tetramethylindocarbocyanine perchlorate) injection into the lateral ventricle (LV) of early postnatal mice demonstrated that NG2$^+$/EGFP$^+$ progenitors migrate from the SVZ through the RMS into the OB. Moreover, fluorescence-activated cell-sorting-purified NG2$^+$/CNP–EGFP$^+$ or NG2$^+$/β-actin–enhanced yellow fluorescent protein-positive (EYFP$^+$) progenitors transplanted into the early postnatal LV displayed extensive rostral and caudal migration. EYFP$^+$ or EGFP$^+$ graft-derived cells within the RMS were DLX$^+$/Er81$^+$ or Nkx2.2$^+$, migrated to the OB, and differentiated to interneurons and oligodendrocytes. In the subcortical white matter (SCWM), grafted cells differentiated to either oligodendrocytes or astrocytes. Transplantation of NG2$^+$/EYFP$^+$ progenitors selectively purified from the SVZ showed that these cells were migratory and generated glia and neurons in the OB, hippocampus, and striatum. In contrast, cortical, OB, or cerebellar NG2$^+$ cells had a very limited migratory potential and gave rise to glia in the SCWM and striatum. Our findings indicate region-specific differences between NG2$^+$ progenitor cells and show that NG2$^+$ cells can migrate throughout the RMS and contribute to both gliogenesis and neurogenesis in the postnatal OB.

Key words: **CNP–EGFP transgenic mice; neural progenitor; oligodendrocyte; interneuron; cell migration; rostral migratory stream**

Introduction

The subventricular zone (SVZ) is a source of new neurons and glia throughout postnatal development into adulthood (Levison and Goldman, 1993; Doestch et al., 1999; Temple, 2001). Neural progenitors of the SVZ are mitotically active and are restricted to different cellular compartments specialized for distinct cell lineages (Levison and Goldman, 1993; Zerlin et al., 1995; Lim et al., 1997). The anterior SVZ (aSVZ) contains progenitor cells that migrate into the rostral migratory stream (RMS), to give rise to neurons in the olfactory bulb (OB) (Doetsch et al., 1999; Temple, 2001; Coskun and Luskin, 2002; Carleton et al., 2003). Conversely, gliogenesis occurs predominantly from the posterior SVZ (Levison and Goldman, 1993; Goldman, 1995; Marshall and Goldman, 2002; Zerlin et al., 2004); it is not yet determined whether neural progenitors from the aSVZ can generate glial cells in the OB.

The combined use of retrovirus infection into the SVZ and time-lapse microscopy revealed distinct distribution and migration patterns for neuronal and glial precursors, and rostral migration of glial precursors was not observed (Suzuki and Goldman, 2003). In agreement with these findings, transplantation of SVZ cells into the lateral ventricle (LV) of perinatal mice demonstrated generation of neurons in the OB and oligodendrocytes in the subcortical white matter (SCWM), with no oligodendrogenesis occurring in the OB (Spassky et al., 2001). The same study concluded that oligodendrocytes in the OB originate from local progenitors that differentiate during forebrain development (Spassky et al., 2001).

In contrast to these findings, recent evidence indicates the existence of multipotent precursors in the RMS capable of giving rise to neurons, oligodendrocytes, and astrocytes (Gritti et al., 2002). These cells have the tendency to generate more oligodendrocytes than neurons or astrocytes (Gritti et al., 2002). Further-

Received Aug. 30, 2004; revised Oct. 11, 2004; accepted Oct. 14, 2004.

This work was supported by National Institutes of Health (NIH) Grant R01NS045702 (V.G.), by the Wadsworth Foundation (V.G.), and by NIH–Mental Retardation and Developmental Disabilities Research Center Grant P30HD40677. We are very grateful to Dr. L.-J. Chew for breeding and maintenance of the CNP–EGFP mice. We thank Dr. Tom Jessel (Columbia University, New York, NY) for the gift of the anti-Er81 antibody. We thank W. King (The William and Shirley Howard Hematopoetic Stem Cell Laboratory, Children's Research Institute, Children's National Medical Center, Washington, DC) and Dr. R. Ruffner (Center for Microscopy and Image Analysis, George Washington University School of Medicine, Washington, DC) for assistance with fluorescence-activated cell sorting and acquisition of confocal images, respectively. We also thank Drs. S. Belachew, L.-J. Chew, T. Haydar, and D. Panchision for discussion and critical comments on this manuscript.

Correspondence should be addressed to Dr. Vittorio Gallo, Center for Neuroscience Research, Children's Research Institute, Children's National Medical Center, Washington, DC 20010. E-mail: vgallo@cnmcresearch.org.

DOI:10.1523/JNEUROSCI.3572-04.2004

 0270-6474/04/2410530-12$15.00/0

more, separate studies have shown that experimentally induced demyelination promotes the proliferation and mobilization of progenitors that populate the OB to generate mature oligodendrocytes (Nait-Oumesmar et al., 1999; Picard-Riera et al., 2002). Finally, polysialic acid (PSA)–neural cell adhesion molecule-positive (NCAM$^+$) precursor cells transplanted into the LV of wild-type or *shiverer* mice displayed rostral migration and generated oligodendrocytes in the OB (Vitry et al., 2001).

The SVZ progenitor population that gives rise to OB interneurons has been characterized recently based on the expression of the ETS domain transcription factor Er81 and Distalless-related homeobox (DLX) proteins (Stenman et al., 2003). Expression of Er81 distinguishes these progenitors from a population of Islet1$^+$ precursors that are also present in the SVZ but give rise to striatal projection neurons (Stenman et al., 2003). The lineage relationship between the Er81$^+$ neuronal progenitors and other precursors in the SVZ (Doetsch et al., 1999; Capela and Temple, 2002; Aguirre et al., 2004) is still undefined.

We have shown recently that cells expressing the proteoglycan NG2 represent a major multipotential progenitor population of the SVZ that gives rise to oligodendrocytes and interneurons (Belachew et al., 2003; Aguirre et al., 2004). In the present study, we investigated whether NG2-expressing cells of the SVZ also contribute to neurogenesis and oligodendrogenesis in the perinatal OB.

Materials and Methods

Transgenic mice. The 2′,3′-cyclic nucleotide 3′-phosphodiesterase (CNP)–enhanced green fluorescent protein (EGFP) and β-actin–enhanced yellow fluorescent protein (EYFP) transgenic mice (Tg Actb EYFP; stock number 003772; JAX Mice, Bar Harbor, ME) have been described previously (Yuan et al., 2002; Belachew et al., 2003; Aguirre et al., 2004). All animal procedures were performed according to the Institutional Animal Care and Use Committee, Children's National Medical Center, and National Institutes of Health guidelines.

Fluorescence-activated cell sorting. Brains were dissected out from postnatal day 2 (P2) to P4 CNP–EGFP mice or P2–P4 β-actin–EYFP mice and transferred to ice-cold HBSS (Invitrogen, San Diego, CA) containing 26 mM HEPES, 0.3% glucose, and 0.75% sucrose. Cells were dissociated in HBSS containing 0.1% trypsin and 100 U/ml DNase I (Sigma, St. Louis, MO) for 20 min at room temperature. The tissue was then transferred to HBSS containing 0.7 mg/ml trypsin inhibitor (Sigma) and triturated with a fire-polished Pasteur pipette. Cell suspensions were analyzed for light forward and side scatter using a FACStar Plus instrument (Beckton Dickinson, Franklin Lakes, NJ). For double NG2$^+$/EGFP$^+$ and NG2$^+$/EYFP$^+$ fluorescence-activated cell-sorting (FACS) analysis, cell suspensions were incubated with appropriate primary antibodies (see below) (Aguirre et al., 2004) and then with R-phycoerythrin (R-PE) conjugated secondary antibodies (Caltag, Burlingame, CA). For NG2$^+$ cell isolation from different brain areas, the SVZ, cortex, OB, and cerebellum were microdissected from 250-μm-thick coronal sections of P2–P4 brains, and cells were dissociated as described above.

Neurosphere preparation and differentiation. The SVZ was microdissected from 250-μm-thick coronal sections of P8 CNP–EGFP brains or β-actin–EYFP mice. Cells were cultured for the neural stem cell colony-forming (neurosphere) assay (Reynolds and Weiss, 1992; Aguirre et al., 2004). FACS-purified SVZ NG2$^+$/EGFP$^+$ or NG2$^+$/EYFP$^+$ cells were seeded at a density of 10 viable cells/μl on uncoated 24-well plates (BD-Falcon, Franklin Lakes, NJ) and grown in stem cell medium (SCM) (Stem Cell Technologies, Vancouver, British Columbia, Canada) for 6 d *in vitro* (DIV) with a daily addition of 20 ng/ml epidermal growth factor (EGF; Upstate, Charlottesville, VA). Primary neurosphere colonies were subcloned by mechanical dissociation in SCM with EGF. Cells were replated at a density of 10 cells/μl on uncoated 24-well plates. Stem cell self-renewal was assessed after an additional 6 DIV. For differentiation experiments, single neurosphere colonies were transferred to individual wells of a 24-well culture plate precoated with 0.1 mg/ml D-polyornithine and laminin (2 μg/ml; Invitrogen) in SCM with 1% FBS and 10 ng/ml BDNF (Upstate). Cells were processed by immunocytochemistry after 6 DIV (Aguirre et al., 2004).

Reverse transcription-PCR. RNA was isolated from P8 FACS-purified NG2$^+$/EGFP$^+$ cells or from neurospheres cultured for 4 d in differentiation medium using Trizol (Invitrogen). RNA (1 μg) from each sample was reverse transcribed using the SuperScript First-Strand cDNA Synthesis kit (Invitrogen). The mouse gene-specific primers used were obtained from Integrated DNA Technologies (Coralville, IA). The sequences were as follows: Er81, sense 5′-CAGAGATCTGGCTCATGATTCAG-3′, antisense 5′-AAAATGCAGCCTTCTGTTCTGC-3′; actin, sense 5′-CGTGGGCCGCCCTAGGCACCA-3′, antisense 5′-AACATGCAGCCTTCTGTTCTGC-3′. Genes were amplified by denaturation at 94°C for 1 min, annealing at 60°C for 1 min, and extension at 72°C for 1 min for 35 cycles. PCR products were resolved by 1.2% agarose gel electrophoresis and visualized by ethidium bromide staining.

Immunocytochemistry. For cell sorting, cell suspensions were incubated with anti-NG2 antibody (1:1000; Chemicon, Temecula, CA) in DMEM (Invitrogen) plus 10% FCS for 30 min at 4°C. After three washes with DMEM, cells

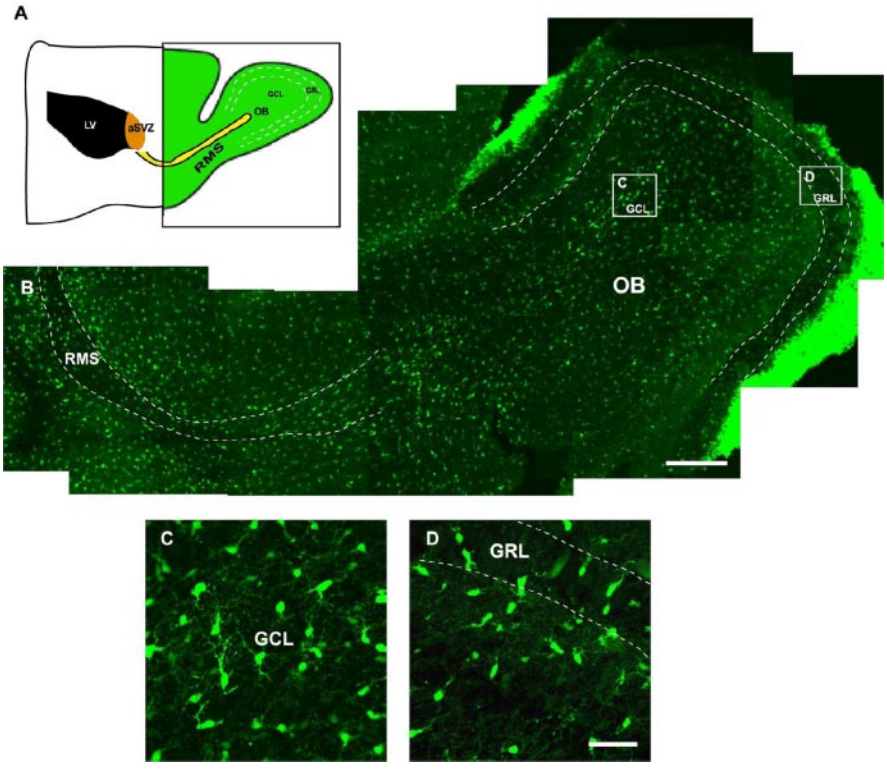

Figure 1. EGFP$^+$ cells are present in the RMS and OB of the postnatal CNP–EGFP mouse. *A*, Schematic drawing of a parasagittal section of the postnatal mouse forebrain. The green-shaded area is shown in *B*. *B*, Confocal reconstruction of the RMS and OB from a parasagittal section obtained from a P8 CNP–EGFP mouse brain. A large number of EGFP$^+$ cells are present in the RMS and in the OB. *C*, *D*, High-magnification images obtained from the boxed areas in *B*. Note the higher density of EGFP$^+$ cells in the GCL than in the GRL. White dotted lines delineate the boundaries of the RMS and the boundaries between the GCL and GRL of the OB. Scale bars: *B*, 300 μm; *C*, *D*, 50 μm.

were incubated with the secondary antibody (200 ng/10^6 cells; R-PE; Caltag) in 2 ml of medium for 15 min at 4°C. For immunocytochemistry, cell cultures were processed as described previously (Yuan et al., 2002; Aguirre et al., 2004) with the following primary antibodies, at a dilution of 1:500: anti-panDLX (from G. Panganiban, University of Wisconsin Madison, Madison, WI), TUJ1 (BabCo, Berkeley, CA), anti-GFAP (Sigma), and anti-GAD-67 rabbit polyclonal (Chemicon). Anti-O4 (mouse monoclonal IgM), anti-Er81 (provided by S. Morton and T. Jessel, Columbia University, New York, NY), and anti-GABA (Sigma) were used at a dilution of 1:50, 1:5000, and 1:1000, respectively.

Immunohistochemistry. Freshly cut, floating tissue sections (50 μm) from P8 mice were prepared as described previously (Yuan et al., 2002; Aguirre et al., 2004). Primary antibody dilutions were as follows: 1:50 for anti-Nkx2.2 (Developmental Studies Hybridoma Bank, Hybridoma Bank, Iowa City, IA); 1:500 for anti-NG2 (Chemicon), anti-Ki67 (Novocastra, Newcastle, UK), anti-CNP and anti-MBP (Sternberger Monoclonal Incorporated, Lutherville, MD), anti-DLX (from G. Panganiban), anti-neuronal-specific nuclear protein (NeuN) (Chemicon), anti-GFP (Clontech), and anti-GFAP (Sigma); 1:1000 for anti-GAD-67 (Chemicon), anti-doublecortin (DC; Chemicon), and anti-nestin (Chemicon). Anti-Er81 (from S. Morton and T. Jessel) was used at a dilution of 1:5000.

Injection of fluorescent tracer. To examine the migration of endogenous CNP–EGFP$^+$ cells from the SVZ *in vivo*, 1,1′-dioctadecyl-3,3,3′,3′-tetramethylindocarbocyanine perchlorate (DiI) (1 mg/ml in 100% methanol; diluted 1:5 in 10% sucrose; Molecular Probes, Eugene, OR) was injected into the LV of P3–P4 mice. Glass micropipettes were backfilled with the DiI solution (1 μl) and directed to the LV by a micromanipulator (Harvard Instruments, Murrieta, CA). Brain tissue of injected mice was then analyzed by immunohistochemistry at 4 d, 1 week, and 3 weeks after DiI injection.

Transplantation and analysis of grafted cells. Wild-type P2–P4 FVB/NxCB6 pups were used as recipients. FACS-purified NG2$^+$/EGFP$^+$ or NG2$^+$/EYFP$^+$ donor cells were prepared from P2–P4 CNP–EGFP or β-actin–EYFP transgenic mice, respectively, as described previously (Aguirre et al., 2004). For experiments in which NG2$^+$ cells were purified from different brain regions and transplanted, cells were isolated from P6–P8 donors to allow accurate microdissection of the tissues. For migration and anatomical distribution studies, mice were maintained for 4 d after the injection and processed for immunohistochemistry. For subsequent anatomical distribution and differentiation analyses of the grafted cells, mice were killed 2–4 weeks after the injection. Grafted NG2$^+$/EGFP$^+$ and NG2$^+$/EYFP$^+$ cells were readily visible under confocal microscopy in unstained tissue, using a 488 nm laser-line excitation. An anti-GFP rabbit polyclonal antibody (IgG; 1:500; BDClontech) was also used to confirm NG2$^+$ cell differentiation by immunohistochemistry (Aguirre et al., 2004). In three different experiments, we quantified the percentage of total transplanted EYFP$^+$ cells found in the striatum, cortex, SCWM, RMS, hippocampus, and OB. For analysis of cell differentiation 3 weeks after transplantation, NeuN, O4, and GFAP antibodies were used as cell markers to identify neurons, oligodendrocytes, and astrocytes, respectively. Ki67 antibody (1:500; Novocastra) was used to assess cell proliferation.

Microscopy and cell counting. A BX60 fluorescence inverted microscope (Olympus, Melville, NY) was used to visualize immunofluorescence in cultured cells derived from neurospheres. Images were acquired using a 40× objective. For analysis in tissue sections, an MRC 1024 confocal laser-scanning microscope (Bio-Rad, Hercules, CA) equipped with a krypton–argon laser and an Olympus IX-70 inverted microscope were used to image localization of FITC (488 nm laser-line excitation; 522/35 emission filter), Texas Red (568 nm excitation; 605/32 emission filter), and Cy5 (647 excitation; 680/32 emission filter). Optical sections (Z = 0.5 μm) of confocal epifluorescence images were acquired sequentially using a 40× [numerical aperture (NA), 1.35], 60× (NA, 1.40), or 100× (NA, 1.35) oil objective with LaserSharp version 3.2 software (Bio-Rad). Confocal Assistant 4.02 and Image J (NIH) software were subsequently used to merge images and orthogonal studies, respectively. Merged images were processed in Photoshop 7.0 with minimal manipulations of contrast.

For cell counting in cultured cells, averages were obtained from three separate sets of cultures. A total of 20 clones per culture were counted. For cell counting of endogenous EGFP$^+$ cells in tissue sections, cells were counted in the SVZ and RMS of P8 mice. We found that 100% of the NG2$^+$ cells were also EGFP$^+$. The analysis of the SVZ and RMS was performed at different rostral levels

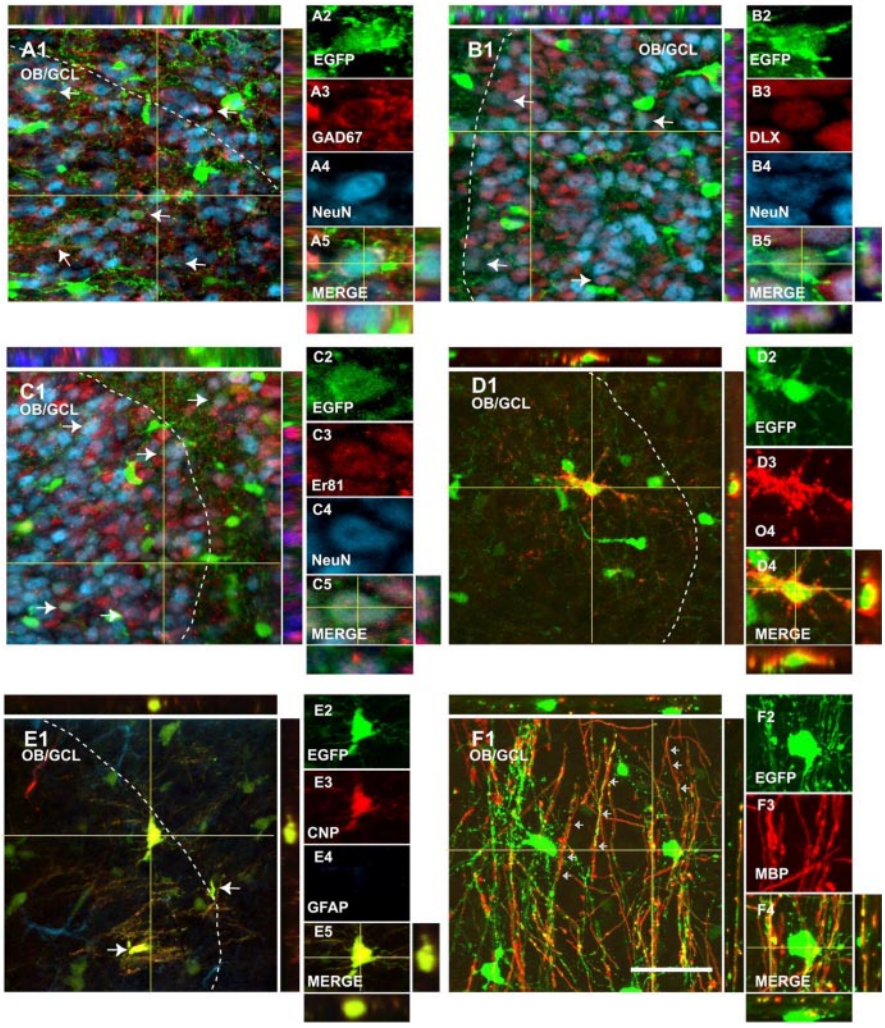

Figure 2. EGFP$^+$ cells in the perinatal OB display neuronal and oligodendroglial phenotypes. Immunostaining of parasagittal sections from a P8 CNP–EGFP mouse brain. A significant percentage of EGFP$^+$ cells expressed the mature neuronal marker NeuN (*A4*, *B4*, *C4*; blue) and the GABAergic interneuron markers GAD-67 (*A3*; red), DLX (*B3*; red), and Er81 (*C3*; red). A percentage of EGFP$^+$ cells expressed the oligodendrocyte markers O4 (*D3*; red), CNP (*E3*; red), and MBP (*F3*; red). White dotted lines delineate the boundaries between the GCL and GRL of the OB. Orthogonal reconstructions of confocal sections in the *z*-axes at the level indicated by the yellow lines are shown in *A1*, *A5*, *B1*, *B5*, *C1*, *C5*, *D1*, *D5*, *E1*, *E5*, *F1*, and *F4*. The individual cells selected for multi-marker illustration are indicated at the intersections of the yellow lines. The arrows represent double positive cells. Scale bar, 50 μm.

Table 1. Characterization of NG2$^+$ cells in the aSVZ and RMS of the perinatal CNP-EGFP mouse

	EGFP$^+$ cells/μm^3	Percentage of EGFP$^+$ cells							
		NG2$^+$/DC$^-$	NG2$^+$/DC$^+$	NG2$^-$/DC$^+$	NG2$^-$/DC$^-$	NG2$^+$/Er81$^+$	NG2$^+$/Nkx2.2$^+$	Er81$^+$/DC$^+$	Nkx2.2$^+$/Er81$^+$
aSVZ	3.1 ± 0.4	72.0 ± 2.6	10.1 ± 1.4	11.7 ± 2.1	16.7 ± 4.4	23.2 ± 1.9	42.2 ± 1.7	7.2 ± 2.3	3.7 ± 2.0
RMS	4.6 ± 0.7	28.7 ± 2.2	1.1 ± 0.4	25.7 ± 5.1	45.7 ± 6.2	18.0 ± 3.2	66.0 ± 4.4	26.3 ± 3.8	0

The analysis of the SVZ and RMS was performed at different rostral levels (Fig. 3, green boxes) in the CNP–EGFP mouse at P8. An average of three to four sections from three different brains (9–12 sections total) were counted for the SVZ and RMS, respectively, to obtain an estimate of the total number of EGFP$^+$ cells. Percentages of EGFP$^+$ cells expressing NG2 proteoglycan, DC, Er81, and Nkx2.2 were estimated by scoring the number of cells double-labeled with the marker in question. Total EGFP$^+$ cells counted ranged between 929 and 1108. Cell counting data in tissue sections are expressed as averages ± SEM.

as shown in Figure 2. An average of three to four sections from three different brains (9–12 sections total) were counted for the SVZ and RMS, to obtain an estimate of the total number of EGFP$^+$ cells. The anatomical distribution of CNP–EGFP$^+$ cells was analyzed in *Z*-series confocal scanning images [20–30 μm thickness; step size, 0.5 μm between successive images of the same field (228 μm^2)]. Percentages of EGFP$^+$ cells expressing different markers were then estimated by scoring the number of cells double-labeled with the markers in question. For counting of cells derived from transplanted whole-brain NG2$^+$/EYFP$^+$ cells, EYFP$^+$ cells were countedas described above in the granular cell layer (GCL) and glomerular layer (GRL) of the OB. Approximately 20–25 sections were counted for each OB to obtain an estimate of the total cells in the entire OB. Cell numbers were obtained from three different experiments (three brains total). Percentages of EYFP$^+$ cells expressing NeuN and O4 were estimated by scoring the number of cells double-labeled with the marker in question. For counting of cells derived from transplanted SVZ and cortical NG2$^+$/EYFP$^+$ cells (see Fig. 9), EYFP$^+$ cells were counted in different brain regions. Cell numbers were obtained by analyzing a total of 144 sections (40 μm thickness) from three different experiments (three different brains). Cell counting data in tissue sections were expressed as averages ± SEM. Statistical analysis was performed by paired *t* test.

Results

EGFP$^+$ cells in the perinatal OB display neuronal and oligodendroglial phenotypes

The postnatal RMS and OB of the CNP–EGFP mouse contain a large number of EGFP$^+$ cells (Fig. 1*B–D*). In the OB, these cells were present at a higher number in the GCL than in the GRL (5.0 ± 0.2 and 3.5 ± 0.1 cells/μm^3, respectively) (Fig. 1*B–D*). We characterized OB EGFP$^+$ cells with neuronal and glial markers. At P8, 34.7 ± 3.4 and 14.1 ± 1.0% of the EGFP$^+$ cells were NeuN$^+$ in the GRL and GCL, respectively (Fig. 2*A*). Of these EGFP$^+$/NeuN$^+$ neurons, 75.0 ± 3.5 and 70.4 ± 3.7 were GAD-67$^+$ in the GRL and GCL, respectively (Fig. 2*A*). Coexpression of NeuN and the transcription factors DLX (Fig. 2*B*) and Er81 (Fig. 2*C*) in virtually all of the NeuN$^+$/EGFP$^+$ neurons confirmed an OB interneuron phenotype. Finally, the OB NeuN$^-$/EGFP$^+$ cells were stained with the oligodendrocyte-specific antibody O4 (Fig. 2*D*) and expressed the CNP and MBP proteins, markers for mature oligodendrocytes (Fig. 2*E*,*F*). These findings indicate that the postnatal OB of the CNP–EGFP mouse contains both EGFP$^+$ neurons and oligodendrocytes and raise the possibility that these cells might have originated from EGFP$^+$ progenitors migrating from the aSVZ through the RMS into the OB (Fig. 1*B*).

NG2$^+$/EGFP$^+$ cells in the perinatal SVZ and RMS express markers of OB interneuron and oligodendrocyte progenitors

We first characterized EGFP$^+$ cells in the P8 RMS by using antibodies for the RMS markers DC (Fig. 3*B*,*E*,*G*) and PSA–NCAM (data not shown) in parasagittal tissue sections. At P8, the EGFP$^+$ cell density in the RMS was 4.6 ± 0.7/μm^3 (Table 1), and a significant percentage of these cells were NG2$^+$ (Fig. 3*C1–C3*, Table 1). NG2$^+$/EGFP$^+$ and NG2$^-$/EGFP$^+$ cells in the RMS displayed the typical morphology of migrating cells (i.e., a small cell body with one or two short cell processes) (Fig. 3). In the RMS, a large percentage of the EGFP$^+$ cells coexpressed NG2 and the oligodendrocyte progenitor (OP) marker Nkx2.2 (Fig. 3*D*, Table 1) (Ericson et al., 1997). Virtually all of the Nkx2.2$^+$ cells were NG2$^+$ (Fig. 3*D*).

Based on the previous finding that 34% of the NG2$^+$/EGFP$^+$ cells in the aSVZ expressed the neuroblast marker DLX (Aguirre et al., 2004), we further characterized the phenotype of the migrating NG2$^+$/EGFP$^+$ and NG2$^-$/EGFP$^+$ cells in the RMS with the OB interneuron marker Er81 and the neuroblast marker DC. We found that ~1% of the total EGFP$^+$ cells in the RMS were NG2$^+$/DC$^+$ and ~26% was NG2$^-$/DC$^+$ (Fig. 3*E*, Table 1). Consistent with these findings, we also observed that 18% of EGFP$^+$ cells in the RMS were NG2$^+$ and expressed the transcription factor Er81, which specifically labels progenitors of OB interneurons in the SVZ (Stenman et al., 2003) (Fig. 3*F*, Table 1). Moreover, we found that ~26% of the EGFP$^+$ cells in the RMS coexpressed Er81 and DC (Fig. 3*G*, Table 1). We observed that virtually 100% of the Er81$^+$/EGFP$^+$ cells in the RMS were also DLX$^+$ (data not shown). Importantly, coexpression of Nkx2.2 and Er81 in RMS EGFP$^+$ cells was never observed. These data indicate that EGFP$^+$ cells in the RMS express both OB interneuron and OP markers.

In the aSVZ, ~10% of the EGFP$^+$ cells were NG2$^+$/DC$^+$ (Fig. 3*H*, Table 1) and 23% were NG2$^+$/Er81$^+$ (Fig. 3*I*, Table 1). Er81 expression in SVZ NG2$^+$/EGFP$^+$ cells was confirmed by reverse transcription (RT)-PCR in FACS-purified P8 cells (see Fig. 5*I*). In the aSVZ, ~40% of the NG2$^+$/EGFP$^+$ cells expressed Nkx2.2 (Table 1); however, only 3% of EGFP$^+$ cells coexpressed Nkx2.2 and Er81 (Table 1).

All of these data obtained in the RMS and aSVZ indicate that EGFP$^+$ cells express both OB interneuron and OP markers. Our results suggest that aSVZ NG2$^+$/EGFP$^+$ progenitors that express Er81 and DC might migrate rostrally into the RMS and downregulate NG2 expression while they differentiate intoEGFP$^+$ OB interneurons. Furthermore, our analysis also indicates that NG2$^+$/EGFP$^+$ progenitors that express NKx2.2 maintain NG2 expression in the RMS and that these progenitors might generate EGFP$^+$ oligodendrocytes in the OB.

NG2$^+$/EGFP$^+$ cells in the perinatal SVZ migrate to the OB

To directly demonstrate that NG2$^+$/EGFP$^+$ progenitors migrate from the SVZ through the RMS into the OB, we first injected DiI into the LV of P3 mice and characterized the DiI-labeled cells 4 d after the injection. Figure 4 shows that many EGFP$^+$ cells that incorporated DiI were found migrating throughout the entire RMS 4 d after the injection (Fig. 4*A-D*,*F*,*G*). At this time, a few DiI$^+$/EGFP$^+$ cells were also found in the OB (Fig. 4*E*). We further characterized the phenotype of DiI$^+$/EGFP$^+$ cells and found that substantial numbers of the cells expressed NG2 (Fig. 4*F*) or DC (Fig. 4*G*).

Additional analysis of the brains at 4 d after the DiI injection confirmed the accuracy of our LV injection protocol, because we were also able to demonstrate the previously described (Suzuki

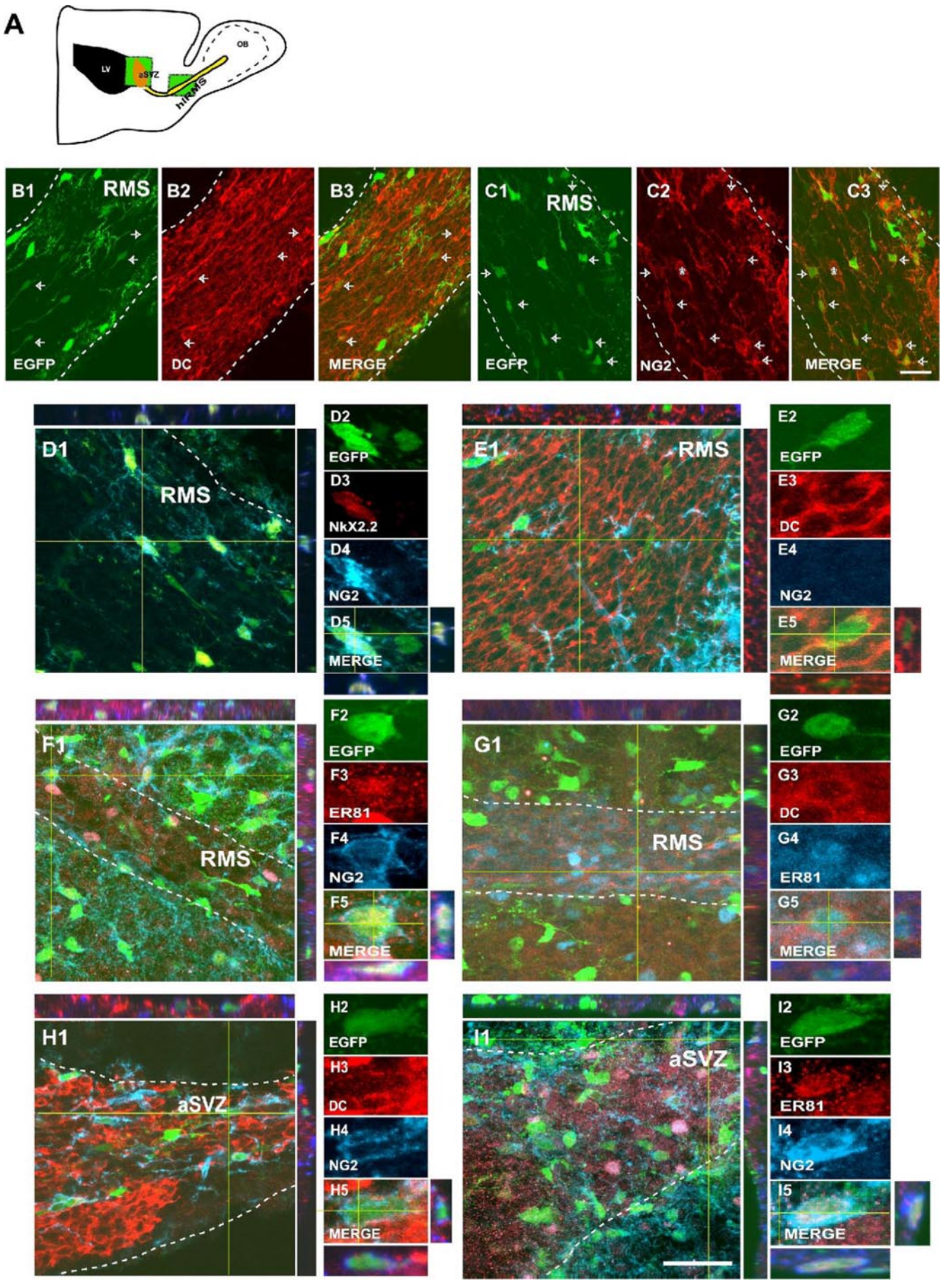
A
LV
aSVZ
OB
hiRMS
B1
RMS
EGFP
B2
DC
B3
MERGE
C1
RMS
EGFP
C2
NG2
C3
MERGE
D1
RMS
D2
EGFP
D3
NkX2.2
D4
NG2
D5
MERGE
E1
RMS
E2
EGFP
E3
DC
E4
NG2
E5
MERGE
F1
RMS
F2
EGFP
F3
ER81
F4
NG2
F5
MERGE
G1
RMS
G2
EGFP
G3
DC
G4
ER81
G5
MERGE
H1
aSVZ
H2
EGFP
H3
DC
H4
NG2
H5
MERGE
I1
aSVZ
I2
EGFP
I3
ER81
I4
NG2
I5
MERGE

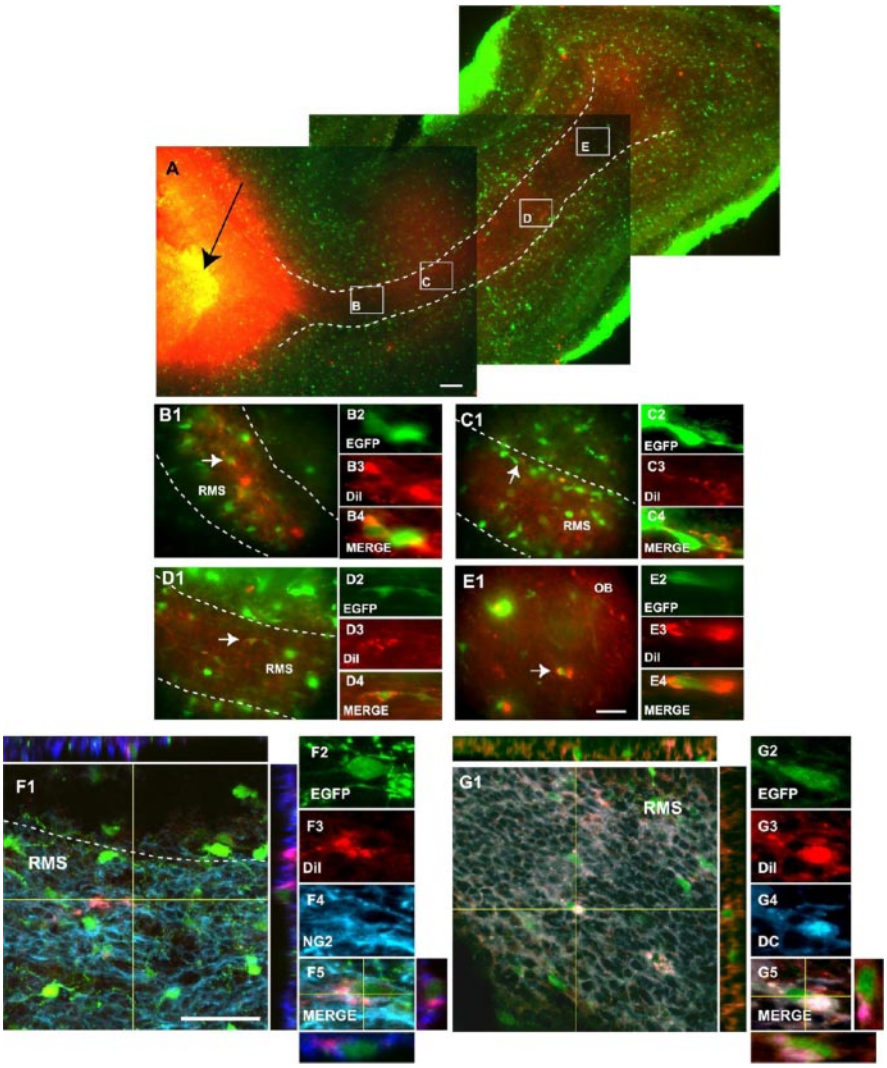

Figure 4. NG2$^+$ cells migrate from the SVZ into the RMS. *A–E*, Reconstruction of a parasagittal brain section of a P8 CNP–EGFP mouse 4 d after DiI injection into the LV (black arrow). EGFP$^+$ cells were found throughout the entire RMS and displayed morphologies of migratory cells. *B–D*, At this time, a small percentage of DiI$^+$/EGFP$^+$ (red/green) cells were also found in the OB (*E*). Boxes in *A* (B–E) are shown at a higher magnification, and individual DiI$^+$/EGFP$^+$-labeled cells (white arrows) are also displayed at a higher magnification. *F*, *G*, A percentage of the migrating DiI$^+$/EGFP$^+$ cells express NG2 (*F4*; blue) and DC (*G4*; blue). White dotted lines represent RMS boundaries. Orthogonal reconstructions of confocal sections in the *z*-axes at the level indicated by the yellow lines are shown in *F1*, *F5*, *G1*, and *G5*. The individual cells selected for multi-marker illustration are indicated at the intersections of the yellow lines. Scale bars: *A*, 300 μm; *B–G*, 50 μm.

and Goldman, 2003) caudal migration of glial progenitors from the SVZ into the SCWM. Supplemental Fig. S1 (available at www.jneurosci.org as supplemental material) shows that a large number of DiI$^+$/EGFP$^+$ cells were found distributed throughout the entire SCWM (Fig. S1*A–D*). Importantly, most of these DiI$^+$/EGFP$^+$ cells maintained NG2 immunoreactivity or were labeled with O4 antibodies, indicating a glial fate (Fig. S1*E*,*F*).

NG2$^+$ cells purified from the SVZ are multipotent and generate OB interneurons and oligodendrocytes *in vitro*

To define the lineage potential of aSVZ NG2$^+$ cells, we generated neurosphere cultures from purified SVZ NG2$^+$ cells and characterized their progeny *in vitro*. Our previous reports indicate that total brain NG2$^+$ cells form neuropheres and behave as multipotent neural stem cells *in vitro* (Belachew et al., 2003; Aguirre et al., 2004). Using P8 striatal-SVZ NG2$^+$/EGFP$^+$ or NG2$^+$/EYFP$^+$ (purified from a β-actin tgEYFP transgenic mouse; stock number 003772; JAX Mice) cells seeded at a clonal density, we observed neurosphere formation after 7 DIV (Aguirre et al., 2004) (data not shown). Dissociation of individual spheres into single cells and replating gave rise to secondary neurospheres, which could then be repassaged several times and frozen, indicating self-renewal (Aguirre et al., 2004) (data not shown).

Secondary and tertiary neurospheres were plated under differentiating conditions to characterize the NG2$^+$ cell-derived progeny. We observed that, similar to NG2$^+$/EGFP$^+$ cells (Aguirre et al., 2004), striatal-SVZ NG2$^+$/EYFP$^+$ (Fig. 5*A–D*) cells were also multipotent. Both types of FACS-purified NG2$^+$ cell populations gave rise to a similar progeny [i.e., 12–16% β-tubulin$^+$ (TUJ1$^+$) neurons, 5–8% O4$^+$ immature oligodendrocytes, and ~50% GFAP$^+$ astrocytes (Belachew et al., 2003)]. Furthermore, NG2$^+$/EYFP$^+$ and NG2$^+$/EGFP$^+$ cell-derived neurospheres comprised OB interneurons, identified with anti-GABA (Fig. 5*E3*,*F3*), anti-GAD-67 (Fig. 5*C3*,*G4*), anti-DLX (Fig. 5*F4*), and anti-Er81 (Fig. 5*D3*,*E4*,*G3*,*H3*) antibodies. We found that the entire population of GABA$^+$ cells was also DLX$^+$ (Fig. 5*F*) and that a large percentage of GABA$^+$ cells also expressed Er81 (Fig. 5*E*). To quantify the percentage of Er81$^+$ OB interneurons generated from SVZ NG2$^+$ cells, we performed double immunolabeling with anti-β-tubulin (TUJ1

←

Figure 3. NG2$^+$ cells in the SVZ and RMS express markers for neuronal progenitors and OPs. *A*, Schematic drawing of a parasagittal section of the postnatal mouse forebrain. The green boxes represent the areas selected for cell imaging and cell counting in the aSVZ and horizontal limb of the RMS (hlRMS). *B1–B3*, EGFP$^+$ cells (green) are found in the hlRMS. The RMS was labeled with anti-DC (red). *C1–C3*, NG2 immunostaining (red) of the RMS demonstrates the presence of NG2$^+$ progenitors in this structure. Arrows represent double positive cells, and the asterisks in *C2* and *C3* represent a blood vessel. *D1–D5*, A percentage of the NG2$^+$ progenitors in the RMS (*D4*; blue) express the OP marker Nkx2.2 (*D3*; red). *E1–E5*, *F1–F5*, A percentage of EGFP$^+$/NG2$^-$ cells (green/blue) express DC (*E3*; red) in the RMS. A percentage of the EGFP$^+$ cells were NG2$^+$ (*F4*; blue) and Er81$^+$ (*F3*; red) in the RMS. *G1–G5*, A population of EGFP$^+$ cells in the horizontal limb of the RMS coexpress DC (*G3*; red) and Er81 (*G4*; blue), markers for OB interneurons. *H1–H5*, *I1–I5*, A percentage of NG2$^+$/EGFP$^+$ cells in the aSVZ express DC (*H3*; red) and Er81 (*I3*; red). White dotted lines delineate the boundaries of the RMS. Orthogonal reconstructions of confocal sections in the *z*-axes at the level indicated by the yellow lines are shown in *E1*, *E5*, *F1*, *F5*, *G1*, *G5*, *H1*, *H5*, *I1*, and *I5*. The individual cells selected for multi-marker illustration are indicated at the intersections of the yellow lines. Scale bar, 50 μm.

clone) and Er81 antibodies. We observed that 83.8 ± 1.6 of the β-tubulin+ cells were also Er81+ (Fig. 5*D*,*H*). Finally, expression of the *Er81* gene in the progeny of NG2+ cells was confirmed by RT-PCR of mRNA purified from NG2+/EGFP+ cell-derived neurospheres (Fig. 5*I*).

Grafted NG2+ cells migrate through the RMS and give rise to interneurons and oligodendrocytes in the OB

To define the lineage potential of NG2+ cells in the OB *in vivo*, we grafted early postnatal (P2–P4) NG2+/EYFP+ and NG2+/EGFP+ cells FACS purified from total brain (Aguirre et al., 2004) into the LV of P3–P4 wild-type mice. After transplantation (24–48 hr), EYFP+ cells were seen attached to the wall of the LV, and a small percentage were found in the RMS, although none were seen in the OB (data not shown). Four days after transplantation (4 DAT), 12.0 ± 2.0% ($n = 2960$ cells) of the grafted EYFP+ cells found in the aSVZ and RMS still coexpressed nestin and Ki67 ($n = 350$ and 329 cells, respectively) (data not shown), indicative of an undifferentiated and proliferative state. At the same age, grafted NG2+/EYFP+ cells displayed a widespread migratory pattern in the brain (data not shown). EYFP+ cells were predominantly incorporated in the SCWM, striatum, hippocampus, fimbria, and OB (see Fig. 9) (data not shown). Migration and differentiation of NG2+ cells in the hippocampus after transplantation has been characterized previously (Aguirre et al., 2004). We focused the present study on the RMS and OB.

At 4 DAT, EYFP+ cells could be found throughout the entire RMS (Fig. 6*A1*), and a significant percentage displayed a typical migrating morphology (Figs. 6*A2*, 7*B1*,*B2*, arrows). At this time, a small percentage of grafted cells had reached the OB (Fig. 6*B1*,*B2*) but maintained the morphology of migratory cells and a nondifferentiated phenotype. Three weeks after transplantation (3 WAT), 18.0 ± 4.1% ($n = 450$ cells) of the total grafted EYFP+ cells were present in the OB and were found distributed in different regions (Fig. 6*B3–B6*), including the GCL (Fig. 6*B3–B6*) and the GRL (Fig. 6*B4*). Importantly, grafted EYFP+ cells found in the OB at this time displayed different morphologies; a significant percentage had a typical neuronal morphology (small cell body and long cell processes) (Fig. 6*B3–B6*, arrows), whereas a higher percentage of cells exhibited a larger cell body and a more complex array of cellular processes, typical of mature oligodendrodocytes (Fig. 6*B4*,*B6*, arrowheads).

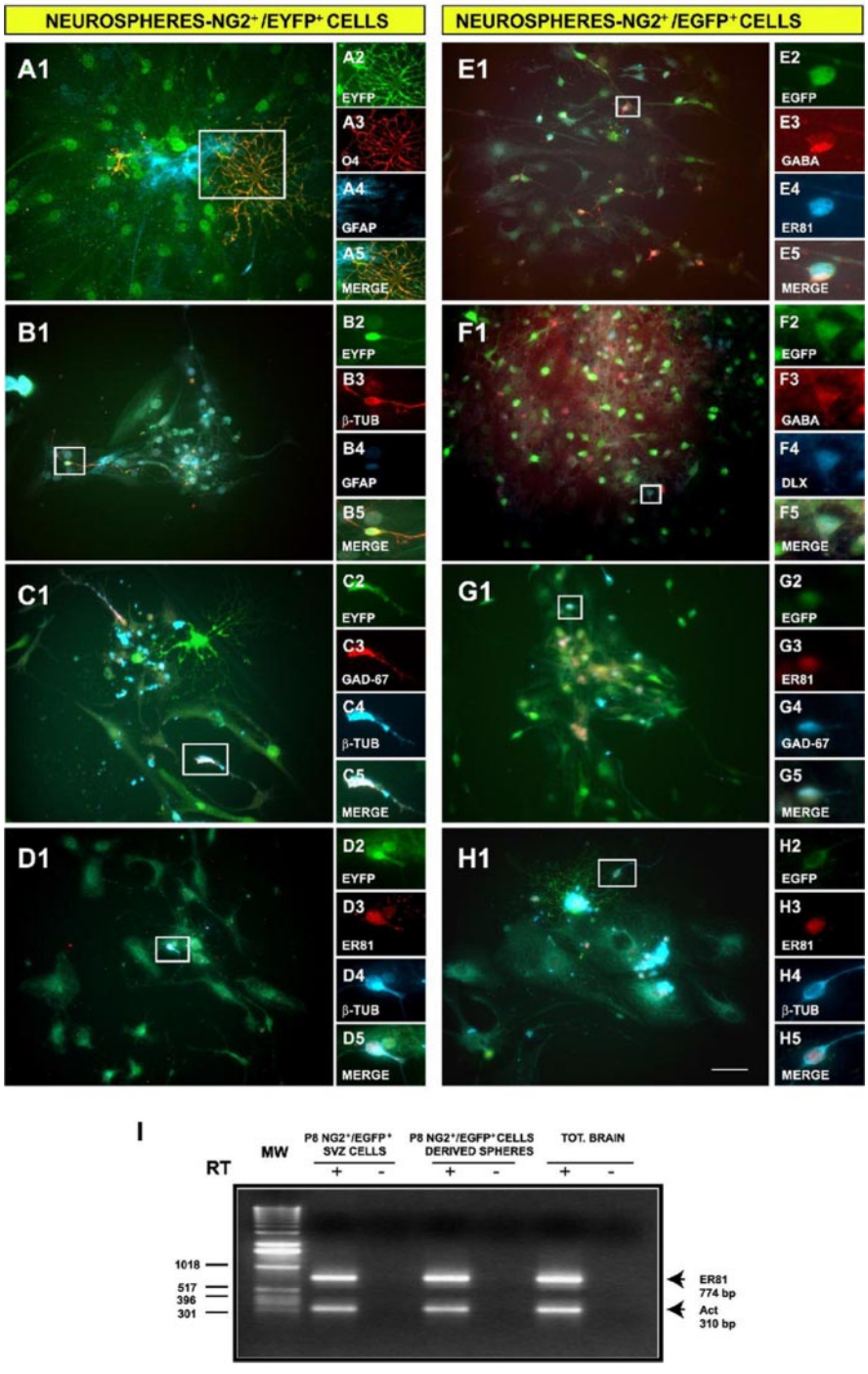

Figure 5. NG2+ cells purified from the SVZ generate OB interneurons and oligodendrocytes *in vitro*. Neurospheres were generated from NG2+/EGFP+ and NG2+/EYFP+ progenitors FACS purified from the SVZ. After plating at a clonal dilution, cells were allowed to differentiate for 6 DIV. *A–D*, Indirect immunofluorescence analysis of their progeny indicated that NG2+/EYFP+ cells are multipotent. Oligodendrodrocytes, astrocytes, and neurons were identified by O4 (*A3*; red), GFAP (*A4*, *B4*; blue), and TUJ1 (*B3*, red; *C4*, *D4*, blue) antibodies, respectively. *C–H*, OB interneurons were identified in NG2+/EYFP+ (*C*, *D*) and in NG2+/EGFP+ (*E–H*) neurospheres using anti-GAD-67 (*C3*, red; *G4*, blue), anti-Er81 (*D3*, *G3*, *H3*, red; *E4*, blue), anti-Dlx (*F4*; blue), and anti-GABA (*E3*, *F3*; red) antibodies. *I*, The transcription factor Er81 is expressed in postnatal (P8) SVZ NG2+/EGFP+ cells (lane 2) and NG2+/EGFP+-derived neurospheres (lane 4), as shown by RT-PCR. −, RNA that was not reverse transcribed was used as a negative control. Scale bar, 50 μm.

We then wanted to characterize the phenotype of the migrating EYFP+ cells in the RMS. EYFP+ cells in the RMS were mostly unipolar or bipolar (Fig. 7*B1*,*B2*, arrows), but we also observed multipolar morphologies (Fig. 7*B1*,*B3*, arrowheads). All graft-derived unipolar/bipolar EYFP+ cells in the RMS were DC+ (Fig. 7*C*). These EYFP+/DC+ cells also expressed early markers of OB

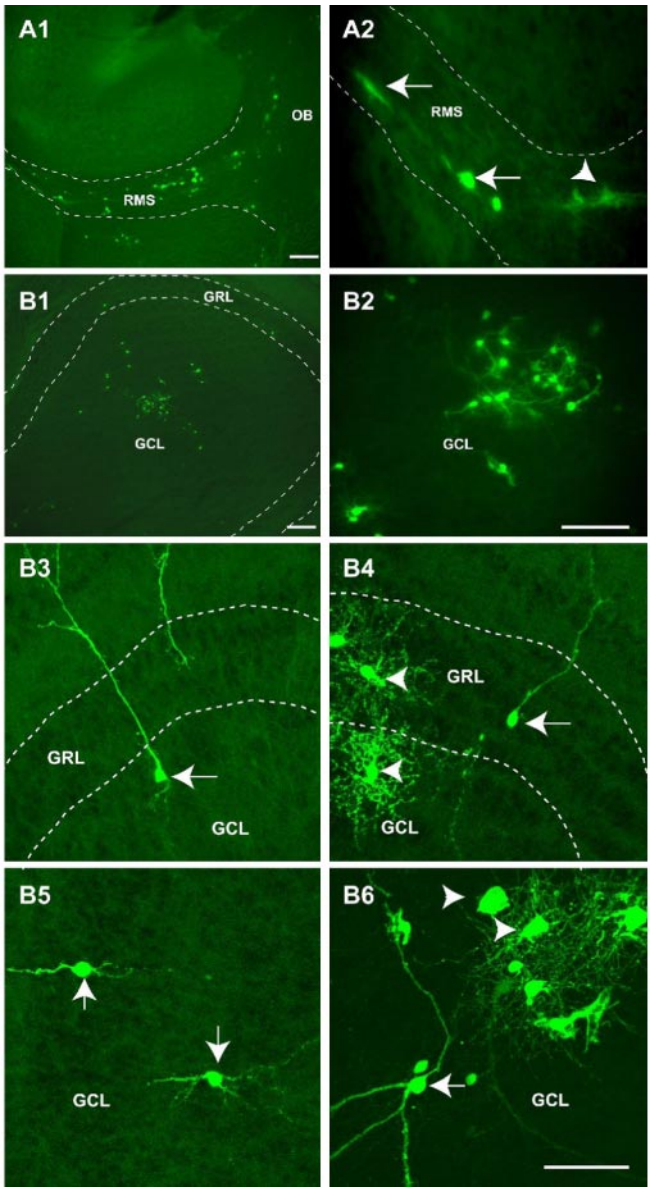

Figure 6. Grafted NG2$^+$/EYFP$^+$ cells migrate rostrally into the RMS to populate the OB. *A*, *B*, NG2$^+$/EYFP$^+$ cells were FACS purified from P3 brains and transplanted in the LV of P3 wild-type host mice. Brains were analyzed at 4 DAT (*A1*, *A2*) and 3 WAT (*B1–B6*). EYFP$^+$ cells were visualized by fluorescence microscopy. *A1*, *A2*, Migrating EYFP$^+$ cells were observed as early as 4 DAT throughout the RMS. *B1–B6*, At 3 WAT, EYFP$^+$ cells were found in the OB and displayed morphological features of neurons (arrows) and oligodendrocytes (arrowheads). These cells were observed both in the GRL and in the GCL. Dotted lines depict the RMS and the GCL of the OB in *A1* and *A2* and in *B1*, *B3*, and *B4*, respectively. Scale bars: *A1*, *B1*, 300 μm; *A2*, *B2*, 200 μm; *B3–B6*, 50 μm.

interneurons, including DLX (Fig. 7*D*) and Er81 (data not shown), but were NG2$^-$. A fraction of graft-derived EYFP$^+$ cells were NG2$^+$ (Fig. 7*E*) and/or O4$^+$ (Fig. 7*F*) but did not express DC (Fig. 7*E*) (data not shown). These cells were mostly multipolar (Fig. 7*E*,*F*) and expressed Nkx2.2 (data not shown). These results indicate that graft-derived EYFP$^+$ cells migrating throughout the RMS are both committed neuronal and committed oligodendrocyte precursors.

At 3 WAT, we found that 8.0 ± 2.1% of the EYFP$^+$ cells in the OB expressed Ki67 (n = 208 cells) (Fig. 8*A*,*B*), indicating that a small percentage of the grafted cells were still proliferative in the OB. To further characterize the fate of the grafted EYFP$^+$ cells in the OB, we performed immunolabeling with several neuronal and glial markers. At 3 WAT, a total of 29% of the EYFP$^+$ cells were neurons, as identified by NeuN staining (Fig. 8*C*, Table 2). These neurons were distributed both in the GCL (19%) and in the GRL (10%) (Table 2). Interestingly, 57% of the total EYFP$^+$ grafted cells displayed the oligodendrocyte marker O4 (Fig. 8*G*, Table 2), and ~30% of the EYFP$^+$ cells expressed markers for differentiated oligodendrocytes, such as CNP (Fig. 8*H*) and MBP (data not shown). Oligodendrocytes were found predominantly in the GCL (52%), and only a small percentage (5%) were found in the GRL (Table 2).

The NG2$^+$ cell-derived neurons in the OB were interneurons, as demonstrated by GAD-67 expression in virtually 100% of the NeuN$^+$/EYFP$^+$ cells found in the OB (Fig. 8*D*). Importantly, graft-derived neurons in the OB maintained expression of DLX (Fig. 8*E*) and Er81 (Fig. 8*F*). We never found EYFP$^+$ cells in the OB that expressed the astroglial marker GFAP.

Transplantation of NG2$^+$/EGFP$^+$ cells isolated from the CNP–EGFP mouse yielded results that were similar to those obtained with NG2$^+$/EYFP$^+$ cells (supplemental Fig. S2, available at www.jneurosci.org as supplemental material). At 4 DAT, NG2$^+$/EGFP$^+$ cells were seen migrating throughout the RMS (supplemental Fig. S2*B1*,*B2*; available at www.jneurosci.org as supplemental material), and 1 week after transplantation, EGFP$^+$ cells were found in both the GCL and the GRL of the OB (supplementary Fig. S2*E*,*F*; available at www.jneurosci.org as supplemental material). A significant percentage of these grafted cells were interneurons, because they expressed DC (Fig. S2*E3*,*F3*; available at www.jneurosci.org as supplemental material), DLX (Fig. S2*F4*), and Er81 (data not shown).

NG2$^+$ cell-derived progenies were also found in the SCWM as a consequence of caudal migration to this brain area. At 3 WAT, 38.0 ± 4.0% (n = 938) of the grafted EYFP$^+$ cells were found in the SCWM. Of these, 19.0 ± 3.2% were Ki67$^+$ (Fig. S3*B*) and 29.0 ± 4.2% expressed the oligodendrocyte marker O4 (data not shown). Furthermore, 26.0 ± 2.0% of the EYFP$^+$ cells expressed markers for mature oligodendrocytes, such as CNP (Fig. S3*C*) and MBP (data not shown). Finally, 8.0 ± 1.2% of the EYFP$^+$ cells expressed the astroglial marker GFAP (Fig. S3*D*). We never found graft-derived EYFP$^+$/NeuN$^+$ neurons in the SCWM (data not shown).

NG2$^+$ cells purified from distinct brain areas exhibit differential migration and lineage potential after grafting

To determine whether NG2$^+$ cells isolated from different brain areas displayed distinct migratory and lineage potentials, we FACS purified and transplanted NG2$^+$/EYFP$^+$ cells from the striatal-SVZ, cerebral cortex, OB, and cerebellum. Cells were isolated from P6–P8 donors to allow accurate microdissection of the tissues. After FACS purification, cells were transplanted into the LV of P3–P4 mouse brains, which were analyzed at 4 DAT to (1) define the extent of migration of the grafted cells and (2) quantify the percentage of total grafted cells found in different brain regions.

Striatal-SVZ NG2$^+$/EYFP$^+$ cells migrated both rostrally and caudally to the OB and to the SCWM (Fig. 9*A1*). Cells derived from SVZ NG2$^+$/EYFP$^+$ progenitors were also found in the striatum. In contrast, cells derived from OB NG2$^+$/EYFP$^+$ progenitors displayed a more restricted migratory potential, because a larger percentage of these cells were found in the fimbria (Fig. 9*B1*). Finally, cortical (Fig. 9*C1*) and cerebellar (data not shown) NG2$^+$/EYFP$^+$ progenitors did not migrate rostrally and altogether exhibited a very limited migration potential. Most of the

cortical and cerebellar EYFP+ cells were found close to the injection site and in the fimbria and striatum (Fig. 9*C1*) (data not shown). Figure 9*A2–C2* shows quantitative data of graft-derived EYFP+ cells found in different regions of the brain at 4 DAT. Significant percentages of EYFP+ cells were found in the hippocampus (6%), RMS (15%), and OB (18%) only after transplantation of SVZ NG2+/EYFP+ cells (Fig. 9*A2*,*B2*). In contrast, SVZ, OB, and cortical NG2+/EYFP+ cells migrated to the SCWM to a similar extent (Fig. 9*A2–C2*). Grafted OB NG2+/EYFP+ cells were found in the RMS (perhaps because of some NG2+/EYFP+ cell contamination from the RMS itself) and within the OB; however, only very rarely were they observed in the hippocampus. The percentage of graft-derived cells found in the fimbria was inversely proportional to the migratory potential of the different NG2+/EYFP+ cell populations (Fig. 9*A2–C2*).

The OB cells derived from SVZ NG2+/EYFP+ cells were either interneurons, based on DLX/NeuN or synaptophysin/NeuN (Fig. 9*D*,*E*) and GAD-67 expression (data not shown), or O4+/CNP+ oligodendrocytes (Fig. 9*F*) (data not shown). Cortical NG2+/EYFP+ cells predominantly generated CNP+ viable oligodendrocytes in the SCWM (Fig. 9*G*) and in the striatum and fimbria (data not shown).

Altogether, these data indicate that striatal-SVZ, OB, and cortical NG2+ cells possess distinct migratory and lineage potentials after transplantation into the perinatal brain.

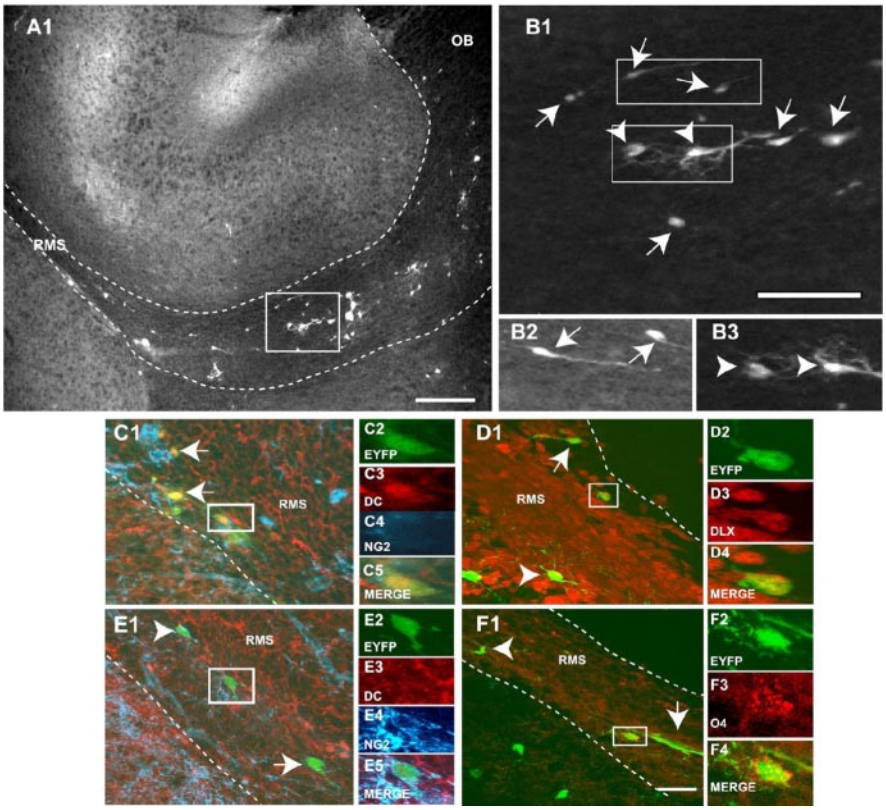

Figure 7. Graft-derived EYFP+ cells are found in the RMS and display different phenotypes. *A1*, EYFP+ cells found in the RMS show a typical unipolar or bipolar migrating morphology, but cells with a bipolar/multipolar OP morphology were also seen. *B1–B3*, A mixed population of unipolar/bipolar (arrows) and multipolar (arrowheads) cells was seen in the RMS. *C*, *D*, Migrating cells in the RMS express the neuroblast markers DC (*C3*; red) and DLX (*D3*; red). *E*, *F*, Multipolar cells in the RMS express NG2 (*E4*; blue) and the oligodendrocyte progenitor marker O4 (*F3*; red) and are negative for DC (*E3*; red). White dotted lines delineate the boundaries of the RMS. The box in *A1* is shown at a higher magnification in *B1*. Boxes in *B1* are shown at a higher magnification in *B2* and *B3*. Scale bars: *A*, 300 μm; *B–F*, 50 μm.

Discussion

To design future strategies aimed at brain regeneration and repair, it is of central importance to study the cellular and developmental properties of neural precursors of the SVZ. This brain area represents a source of neurons and glia from progenitor cells that maintain their cell-cycling potential throughout postnatal development into adulthood (Levison and Goldman, 1993; Zerlin et al., 1995; Lim et al., 1997; Coskun and Luskin, 2002). The identity and cellular properties of the neural stem cells in the SVZ have been studied extensively (Doetsch et al., 1999, 2002; Capela and Temple, 2002; Aguirre et al., 2004); however, the identification of common progenitors that give rise to different classes of neurons and glia *in vivo* is still incomplete, particularly in the early postnatal brain.

In the present study, we provide direct evidence that NG2-expressing progenitor (NG2+) cells of the SVZ can generate GABAergic interneurons and oligodendrocytes in the postnatal OB. We used two distinct transgenic mice, the CNP–EGFP (Yuan et al., 2002) and the β-actin–EYFP mouse (Tg ActbEYFP; stock number 003772), to identify NG2+ cells and their differentiated progeny *in vivo* and *in vitro*. We obtained identical results from both transgenic animals. Our findings in the early postnatal brain indicate the following: (1) the OB contains interneurons and oligodendrocytes that express CNP–EGFP; (2) the RMS contains EGFP+ cells that display properties of committed neuronal (DC+ and Er81+) or oligodendrocyte (NKx2.2+) progenitors; (3) DiI injection into the LV results in the labeling of NG2+/DiI+ progenitors that migrate rostrally and caudally to the OB and the SCWM, respectively; (4) NG2+/EYFP+ and NG2+/EGFP+ progenitor cells transplanted into the LV reproduced the same pattern of migration of endogenous NG2+/DiI+ cells and generated interneurons and oligodendrocytes in the OB; and (5) clonally expanded NG2+ cells purified from the SVZ generated OB GABAergic interneurons and oligodendrocytes *in vitro*.

We have demonstrated recently (Aguirre et al., 2004) that early postnatal NG2+ cells that also express the *CNP* gene in the SVZ display cellular properties described previously for adult type-C cells (Doetsch et al., 1999, 2002; Capela and Temple, 2002) and generate GABAergic interneurons in the postnatal hippocampus (Belachew et al., 2003; Aguirre et al., 2004). We have also shown that NG2+ cells self-renew and express different markers of postnatal/adult neural stem cells, including LeX (Capela and Temple, 2002), the EGF-R (Doetsch et al., 2002), PSA–NCAM (Nguyen et al., 2003), and the transcription factors Olig2, Mash1, and DLX (Doetsch et al., 2002; Doetsch, 2003). In the present study, we demonstrated that the OB interneuron marker Er81 and the neuroblast marker DC (Parmar et al., 2003; Stenman et al., 2003) are also expressed by a significant percentage of SVZ NG2+ cells, indicating a possible lineage relationship between NG2+ progenitors and OB interneurons. This relationship is directly demonstrated by our results obtained by DiI

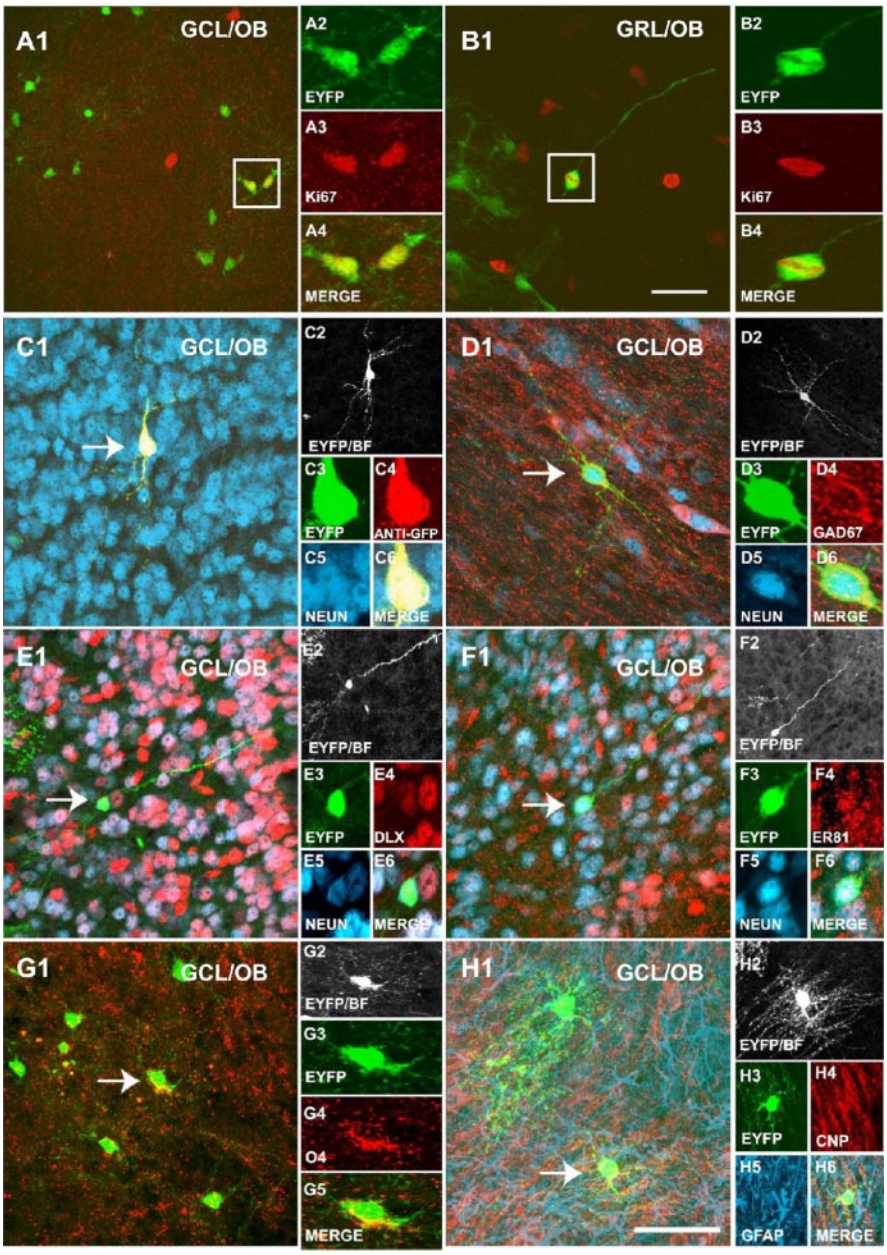

Figure 8. Grafted NG2$^+$/EYFP$^+$ cells differentiate into region-specific interneurons and mature oligodendrocytes in the OB. Tissue analysis was performed at 3 WAT. *A*, *B*, A significant percentage of grafted EYFP$^+$ cells are still proliferative in the OB, as demonstrated by Ki67 staining (*A3*, *B3*; red). *C–F*, Grafted EYFP$^+$ cells display mature OB interneuron markers. EYFP$^+$ cells were stained with anti-NeuN (*C5*, *D5*, *E5*, *F5*; blue), anti-GAD-67 (*D4*; red), anti-Dlx (*E4*; red), and anti-Er81 (*F4*; red). Tissue was also processed for immunohistochemistry with anti-GFP (*C4*; red) to confirm the identity of graft-derived cells. *G1–G5*, Grafted EYFP$^+$ cells were labeled with the oligodendrocyte marker O4 (*G4*; red). *H1–H6*, Grafted EYFP$^+$ cells also displayed a mature oligodendrocyte phenotype, based on CNP protein expression (*H4*; red) and absence of GFAP (*H5*; blue). In *C2*, *D2*, *E2*, *F2*, *G2*, and *H2*, EYFP expression was color converted to black and white to show the full morphology of the grafted cells. The boxes in *A1* and *B1* are shown at a higher magnification in *A2–A4* and *B2–B4*. Arrows indicate cells shown at higher magnification. Scale bars, 50 μm.

labeling of SVZ cells and by grafting of FACS-purified NG2$^+$ cells. With these approaches, we demonstrate that, with a similar time course of a few days, both endogenous and transplanted NG2$^+$ cells migrate from the SVZ into the RMS to generate OB interneurons and oligodendrocytes.

In the SVZ, endogenous DC$^+$/EGFP$^+$ progenitors are either NG2$^+$ or NG2$^-$, but in the RMS, the vast majority of the endogenous DC$^+$/EGFP$^+$ cells are NG2$^-$, indicating that NG2 expression might be downregulated while progenitors migrate from the SVZ into the RMS. This hypothesis is consistent with (1) the previous finding that NG2 expression is downregulated in endogenous and grafted progenitors when they differentiate to GABAergic interneurons in the postnatal hippocampus (Belachew et al., 2003; Aguirre et al., 2004) and (2) the grafting experiments performed in the present study with NG2$^+$/EYFP$^+$ cells, which demonstrate downregulation of NG2 expression in EYFP$^+$ cells that migrate into the RMS.

We FACS purified NG2-expressing progenitors from two distinct transgenic mouse strains (CNP–EGFP and β-actin–EYFP mice) to circumvent possible artifacts attributable to changes in the cellular properties of the progenitor population, which might be caused by promoter activity. Our data clearly indicate that both NG2$^+$/EGFP$^+$ and NG2$^+$/EYFP$^+$ progenitors migrated from the SVZ into the RMS and generated OB interneurons within 2 weeks after transplantation. The neuronal differentiation potential of NG2$^+$ progenitors is linked to the expression of the OB region-specific gene *Er81* and the neuroblast markers DLX and DC, which are present in a significant percentage of NG2$^+$ cells in the SVZ and in the RMS and are maintained in their differentiated progeny in the OB. These results are strongly in agreement with the fate-mapping studies performed by Stenman et al. (2003) in the *Dlx5/6-cre* transgenic mouse, which demonstrated that Er81-expressing cells in the GCL and GRL of the OB derive from progenitors of the SVZ that express DLX.

Based on the finding that postnatal NG2$^+$ cells share molecular and cellular properties of adult type-C cells of the SVZ (Doestch et al., 2002; Aguirre et al., 2004), it is plausible that both oligodendrocytes as well as interneurons of the OB could derive from NG2$^+$/EGFP$^+$ progenitors of the SVZ. In support of this hypothesis, we found that a significant percentage of NG2$^+$/EGFP$^+$ cells in the aSVZ and RMS expressed Nkx2.2, a cellular marker for OPs (Ericson et al., 1997), and many EGFP$^+$ cells in the OB expressed the oligodendrocyte marker CNP protein. Furthermore, transplantation of FACS-purified NG2$^+$ progenitors resulted in the generation of oligodendrocytes in the OB as early as 2 weeks after grafting. The finding that Nkx2.2 and Er81 were not coexpressed in EGFP$^+$ progenitors of the RMS or coexpressed in a very small percentage of EGFP$^+$ cells of the aSVZ (Table 1) indicates that NG2$^+$/EGFP$^+$/Nkx2.2$^+$ and NG2$^+$/EGFP$^+$/Er81$^+$ cells represent two distinct NG2$^+$ progenitor subpopulations. This is confirmed by the observation that in FACS-purified SVZ NG2$^+$/EGFP$^+$ cells, only 5% of the cells coexpressed Nkx2.2 and Er81 (data not shown).

Table 2. Cellular characterization of EYFP+ cells of the OB derived from transplanted NG2+/EYFP+ cells

	Percentage of total EYFP+ in the OB		
	NeuN+	O4+	NI
GCL	19 ± 1	52 ± 2	10 ± 2
GRL	10 ± 2	5 ± 2	3 ± 1

Percentages of EYFP+ cells expressing NeuN and O4 were estimated by scoring the number of cells double-labeled with the marker in question. Numbers indicate the mean and SEM of numbers of EYFP+ cells found in each region of the OB. Cell numbers were obtained from three different experiments (3 brains total), as described in Table 1 and in Materials and Methods. EYFP+ cells were counted in the GCL and GRL of the OB. Total EYFP+ cells counted ranged between 7530 and 8760. NI, Unidentified by either NeuN or O4 antibodies. Cell counting data in tissue sections are expressed as averages ± SEM.

Abundant oligodendrogenesis from NG2+ progenitors was also observed in the SCWM within a few days after grafting in the LV. However, in the same brain area, we also found a significant percentage of GFAP+ astrocytes derived from transplanted NG2+ progenitors. These results are consistent with previous data demonstrating that A2B5+ progenitors isolated from the human fetal brain and transplanted into the white matter of *shiverer* mice gave rise to both oligodendrocytes and astrocytes (Windrem et al., 2004).

OB oligodendrogenesis from SVZ progenitors has been studied previously in different experimental models of demyelination (Vitry et al., 2001; Picard-Riera et al., 2002). In these animal models, it was demonstrated that SVZ progenitor proliferation and migration into the RMS was enhanced in response to experimental autoimmune encephalomyelitis (EAE) or in the *shiverer* mouse. This resulted in a significant increase in oligodendrocyte number in the OB (Vitry et al., 2001; Picard-Riera et al., 2002). Importantly, the SVZ progenitor population recruited for new oligodendrocyte formation was characterized as being PSA–NCAM+/NG2+ or PSA–NCAM+ in the EAE (Picard-Riera et al., 2002) or *shiverer* (Vitry et al., 2001) model, respectively. These properties are consistent with our finding that NG2+/EGFP+ cells in the postnatal SVZ also express PSA–NCAM (Aguirre et al., 2004), although our data indicate that SVZ NG2+ cells also contribute to postnatal oligodendrogenesis in the OB under nonpathological conditions.

Our study indicates that both endogenous and transplanted NG2+/EGFP+ or NG2+/EYFP+ progenitors migrate both rostrally into the RMS and caudally to the SCWM. Rostral migration of neuronal progenitors from the adult SVZ through the RMS to the OB has been widely described (Coskun and Luskin, 2002; Carleton et al., 2003; Suzuki and Goldman, 2003); however, whether OPs could also display the same migration pattern has not been determined. Our analysis in the early postnatal brain demonstrates that endogenous and transplanted NG2+/Nkx2.2+ OPs can migrate through the RMS, as shown previously for NG2+/PSA–NCAM+ SVZ progenitors in EAE mice (Picard-Riera et al., 2002). The validity of these findings is corroborated by the results obtained in the same experiments, which demonstrated that both endogenous NG2+/EGFP+/DiI+ progenitors and transplanted NG2+/EYFP+ cells migrated caudally to the SCWM to generate oligodendrocytes. Caudal migration of OPs to the SCWM has been defined previously by using retroviral injection in the SVZ (Zerlin et al., 2004). Our data obtained with different approaches support

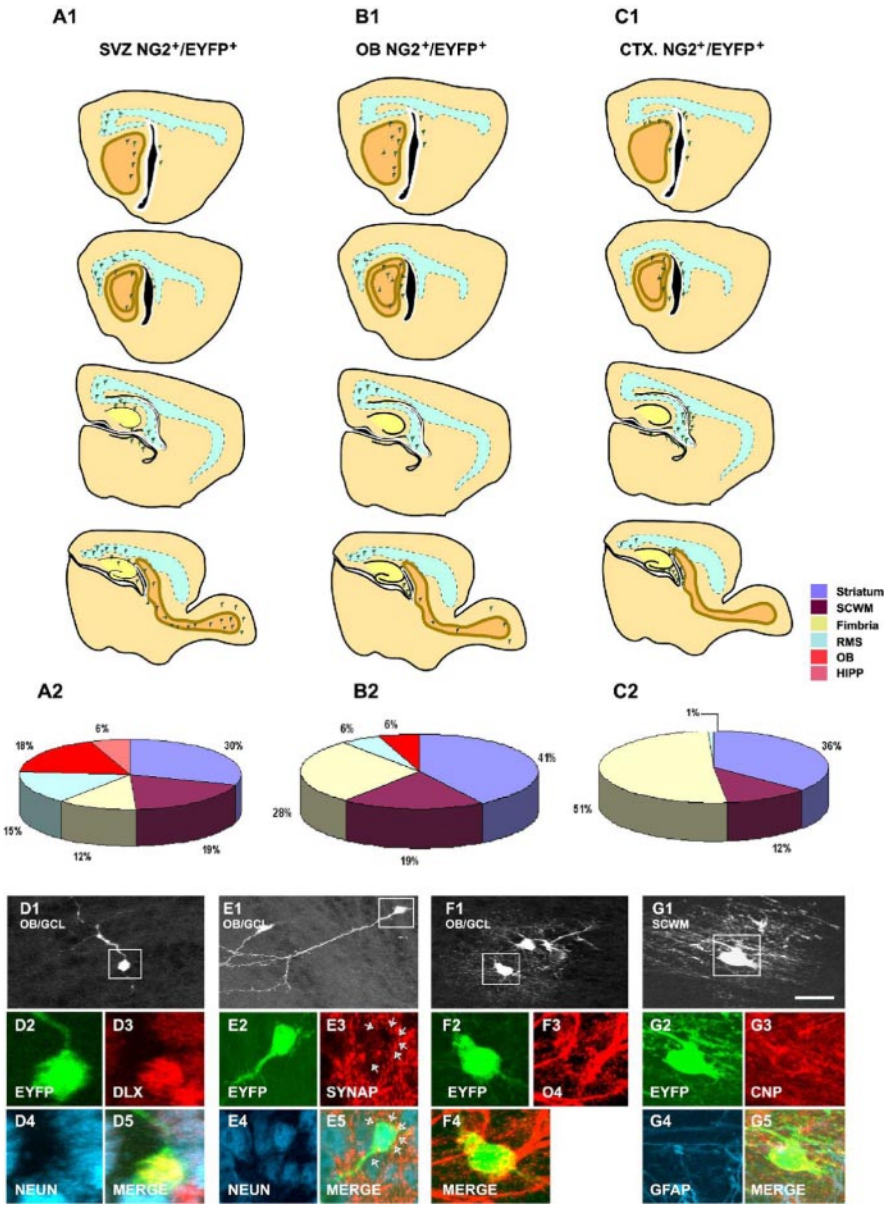

Figure 9. Distinct migratory and lineage potential of NG2+ cells isolated from different brain regions. *A1–C1*, Forebrain diagrams showing representative cellular distributions of striatal-SVZ (*A1*), OB (*B1*), and cortical (*C1*) NG2+/EYFP+ 4 d after grafting in the LV. *A2–C2*, Pies representing the percentages of total grafted cells found in the striatum (purple), SCWM (brown), fimbria (yellow), RMS (blue), OB (orange), and hippocampus (pink) at 4 DAT. *D*, *E*, Representative immunohistochemical characterization of DLX+ (*D3*; red)/NeuN+ (*D4*; blue) or synaptophysin+ (SYNAP; *E3*, red)/NeuN+ (*E4*; blue) OB neurons derived from grafted SVZ NG2+/EYFP+ cells. *F*, Representative immunohistochemical characterization of an oligodendrocyte derived from SVZ NG2+/EYFP+ cells in the OB stained with O4 antibodies (*F3*; red). *G*, Representative immunohistochemical characterization of an oligodendrocyte derived from cortical NG2+/EYFP+ cells in the SCWM stained with anti-CNP antibodies (*G3*; red). Scale bar, 50 μm.

the notion that this is a major migratory pathway of SVZ progenitors that populate the SCWM to generate oligodendrocytes and astrocytes.

To determine whether NG2$^+$ cells of the SVZ were the direct precursors of both interneurons and oligodendrocytes in the OB, we selectively purified these cells from the SVZ of the β-actin–EYFP mouse (1) to analyze their migration pattern and lineage potential after transplantation and (2) to compare their migration pattern and differentiation with other NG2$^+$ cell populations isolated from other brain regions. This analysis confirmed that NG2$^+$ progenitors of the SVZ extensively migrate rostrally and caudally and generate neurons and oligodendrocytes in the OB but only oligodendrocytes and astrocytes in the SCWM. Importantly, OB, cortical, and cerebellar NG2$^+$ cells displayed markedly distinct intrinsic properties *in vivo* (i.e., limited migration and a predominantly glial fate), although cortical NG2$^+$ cells can generate neurons in culture (Chittajallu et al., 2004).

In conclusion, our data demonstrate that the early postnatal aSVZ contains distinct NG2$^+$ cell subpopulations, including NG2$^+$/Er81$^+$/Dlx$^+$/DC$^+$ and NG2$^+$/Nkx2.2$^+$ progenitors. Both subpopulations migrate through the RMS and contribute significantly to neurogenesis and gliogenesis in the OB. Future experiments will further define the heterogeneity of NG2$^+$ progenitors located in different regions of the postnatal and adult brain in terms of their molecular and functional properties and their migration potential.

References

Aguirre AA, Chittajallu R, Belachew S, Gallo V (2004) NG2-expressing cells in the subventricular zone are type C-like cells and contribute to interneuron generation in the postnatal hippocampus. J Cell Biol 165:575–589.

Belachew S, Chittajallu R, Aguirre AA, Yuan X, Kirby M, Anderson S, Gallo V (2003) Postnatal NG2 proteoglycan-expressing progenitor cells are intrinsically multipotent and generate functional neurons. J Cell Biol 161:169–186.

Capela A, Temple S (2002) LeX/ssea-1 is expressed by adult mouse CNS stem cells, identifying them as nonependymal. Neuron 35:865–875.

Carleton A, Petreanu LT, Lansford R, Alvarez-Buylla A, Lledo PM (2003) Becoming a new neuron in the adult olfactory bulb. Nat Neurosci 6:507–518.

Chittajallu R, Aguirre AA, Gallo V (2004) NG2-positive cells in the white and grey matter display distinct physiological properties. J Physiol (Lond), in press.

Coskun V, Luskin MB (2002) Intrinsic and extrinsic regulation of the proliferation and differentiation of cells in the rodent rostral migratory stream. J Neurosci Res 69:795–802.

Doetsch F (2003) A niche for adult neural stem cells. Curr Opin Genet Dev 13:543–550.

Doetsch F, Caille I, Lim DA, Garcia-Verdugo JM, Alvarez-Buylla A (1999) Subventricular zone astrocytes are neural stem cells in the adult mammalian brain. Cell 97:703–716.

Doetsch F, Petreanu L, Caille I, Garcia-Verdugo JM, Alvarez-Buylla A (2002) EGF converts transit-amplifying neurogenic precursors in the adult brain into multipotent stem cells. Neuron 36:1021–1034.

Ericson J, Rashbass P, Schedl A, Brenner-Morton S, Kawakami A, van Heyningen V, Jessell TM, Briscoe J (1997) Pax6 controls progenitor cell identity and neuronal fate in response to graded Shh signaling. Cell 90:169–180.

Goldman JE (1995) Lineage, migration, and fate determination of postnatal subventricular zone cells in the mammalian CNS. J Neurooncol 24:61–64.

Gritti A, Bonfanti L, Doetsch F, Caille I, Alvarez-Buylla A, Lim DA, Galli R, Verdugo JM, Herrera DG, Vescovi AL (2002) Multipotent neural stem cells reside into the rostral extension and olfactory bulb of adult rodents. J Neurosci 22:437–445.

Levison SW, Goldman JE (1993) Both oligodendrocytes and astrocytes develop from progenitors in the subventricular zone of postnatal rat forebrain. Neuron 10:201–212.

Lim DA, Fishell GJ, Alvarez-Buylla A (1997) A postnatal mouse subventricular zone neuronal precursors can migrate and differentiate within multiple levels of the developing neuraxis. Proc Natl Acad Sci USA 94:14832–14836.

Marshall CA, Goldman JE (2002) Subpallial dlx2-expressing cells give rise to astrocytes and oligodendrocytes in the cerebral cortex and white matter. J Neurosci 22:9821–9830.

Nait-Oumesmar B, Decker L, Lachapelle F, Avellana-Adalid V, Bachelin C, Van Evercooren AB (1999) Progenitor cells of the adult mouse subventricular zone proliferate, migrate and differentiate into oligodendrocytes after demyelination. Eur J Neurosci 11:4357–4366.

Nguyen L, Rigo JM, Malgrange B, Moonen G, Belachew S (2003) Untangling the functional potential of PSA-NCAM-expressing cells in CNS development and brain repair strategies. Curr Med Chem 10:2185–2196.

Parmar M, Skogh C, Englund U (2003) A transplantation study of expanded human embryonic forebrain precursors: evidence for selection of a specific progenitor population. Mol Cell Neurosci 23:531–543.

Picard-Riera N, Decker L, Delarasse C, Goude K, Nait-Oumesmar B, Liblau R, Pham-Dinh D, Evercooren AB (2002) Experimental autoimmune encephalomyelitis mobilizes neural progenitors from the subventricular zone to undergo oligodendrogenesis in adult mice. Proc Natl Acad Sci USA 99:13211–13216.

Reynolds BA, Weiss S (1992) Generation of neurons and astrocytes from isolated cells of the adult mammalian central nervous system. Science 255:1707–1710.

Spassky N, Heydon K, Mangatal A, Jankovski A, Olivier C, Queraud-Lesaux F, Goujet-Zalc C, Thomas JL, Zalc B (2001) Sonic hedgehog-dependent emergence of oligodendrocytes in the telencephalon: evidence for a source of oligodendrocytes in the olfactory bulb that is independent of PDGFRalpha signaling. Development 128:4993–5004.

Stenman J, Toresson H, Campbell K (2003) Identification of two distinct progenitor populations in the lateral ganglionic eminence: implications for striatal and olfactory bulb neurogenesis. J Neurosci 23:167–174.

Suzuki SO, Goldman JE (2003) Multiple cell populations in the early postnatal subventricular zone take distinct migratory pathways: a dynamic study of glial and neuronal progenitor migration. J Neurosci 23:4240–4250.

Temple S (2001) The development of neural stem cells. Nature 414:112–117.

Vitry S, Avellana-Adalid V, Lachapelle F, Evercooren AB (2001) Migration and multipotentiality of PSA-NCAM+ neural precursors transplanted in the developing brain. Mol Cell Neurosci 17:983–1000.

Windrem MS, Nunes MC, Rashbaum WK, Schwartz TH, Goodman RA, McKhann II G, Roy NS, Goldman SA (2004) Fetal and adult human oligodendrocyte progenitor cell isolates myelinate the congenitally dysmyelinated brain. Nat Med 10:93–97.

Yuan X, Chittajallu R, Belachew S, Anderson S, McBain CJ, Gallo V (2002) Expression of the green fluorescent protein in the oligodendrocyte lineage: a transgenic mouse for developmental and physiological studies. J Neurosci Res 70:529–545.

Zerlin M, Levison SW, Goldman JE (1995) Early patterns of migration, morphogenesis, and intermediate filament expression of subventricular zone cells in the postnatal rat forebrain. J Neurosci 15:7238–7249.

Zerlin M, Milosevic A, Goldman JE (2004) Glial progenitors of the neonatal subventricular zone differentiate asynchronously, leading to spatial dispersion of glial clones and to the persistence of immature glia in the adult mammalian CNS. Dev Biol 270:200–213.